



Linear Driving Force Model for Adsorption onto Activated Carbon Monolith

DARMADI¹, THOMAS S.Y. CHOONG^{2,*}, CHUAH, T.G.²,
ROBIAH YUNUS², Y.H. TAUFIQ YAP³

¹Department of Chemical Engineering, Faculty of Engineering Syiah Kuala University,
Banda Aceh, Indonesia

²Department of Chemical and Environmental Engineering, Faculty of Engineering
Universiti Putra Malaysia, 43400 UPM Serdang, Selangor D.E., Malaysia

³Department of Chemistry, Faculty of Science, Universiti Putra Malaysia, 43400 UPM Serdang,
Selangor D.E., Malaysia

* Corresponding author: Phone: +60389466293, fax.: +6086567021, e-mail: tsyc2@eng.upm.edu.my

Abstract. A mathematical model on carbon coated monolith using the linear driving force model is developed. The computer program is written in MATLAB and simulation using data from [4] for cell density 200 cpsi was used to study the effect of different variables on breakthrough profiles. The result showed that the breakthrough curve of the monolith is very sharp. Because of its open structure and lower pressure drop, monolith is an attractive alternative internal for separation. Copyright © 2006 Teknik Kimia UNSYIAH

Keywords: Adsorption, modeling, simulation, carbon coated monolith, breakthrough

INTRODUCTION

Porous carbon materials or activated carbons have been in use for many years as solid adsorbent in fields of adsorption because of their large adsorptive capacity and low cost. These activated carbons can be produced from natural source or polymer. Different types of activated carbon provide different characteristics and capacities. Activated carbons from natural source have non-uniform pore size distribution. In order to produce activated carbons which provide controlled pore size distribution, carbon derived from polymer is usually used. Applied forms of activated carbon used commonly are in the shape of powder or granule.

The development of controlled porous carbon derived from polymeric materials such as poly(furfuryl alcohol), furfuryl alcohol, furan, etc. is targeted to produce

carbon with the desired pore structure. Poly(ethylene glycol) as pore former added to poly(furfuryl alcohol) prior to pyrolysis was used to create mesoporosity activated carbon (Lafatis *et al.*, 1991). The application of activated carbon products, in general, is implemented in packed bed column. Activated carbon applied in packed bed has disadvantages, *i.e.*, high pressure drop associated with the flow through packed bed media, channeling, hot spot, and runaway behavior for extremely exothermic reaction. Another problem associated with packed bed is the entrainment of particles in the flow stream. The monolithic column is an attractive alternative system to eliminate the problems mentioned previously for packed column.

The activated carbon monolith structure is known to have very high geometric surface area to volume ratio, and has very open structure. It can be located in

a vertical and horizontal position or in mobile system without losing shape and is easier to be scaled up due to its simple design and uniform flow distribution [1]. Other advantages are the accessible surface area of the activated carbon monolith is larger than that of the packed column. Monolithic catalyst structures have been widely applied in single-phase flow such as automotive emission control, selective catalytic reduction of NO_x [3-5], adsorption of gas [2-6], and selective oxidation. More recently, the opportunities in multiphase catalytic processes have been recognized, leading to increase research interest in this area. These processes include hydrogenation, oxidation, and decomposition reactions [3,4,7]. The production of H₂O₂ [8] is an industrial application example.

The objective of this work is to develop an linear driving force adsorption model to simulate the effect of the total lengths of the monoliths and velocities of feeds on the breakthrough performance for linear isotherm.

Modeling

The mathematical model on monolithic column is developed on the basis of one single square channel with a flat carbon coating on the wall. The sketch of monolithic structure is illustrated in Figure 1, where R_1 and R_2 are the radius of channel's wall and the radius of the channel, respectively.

The following assumptions are applied in the mathematical model development:

- The monolith channel is a square by applying diameter equivalent with inside radius R_2
- No variation of the mass transfer parameters and physicochemical properties along the monolithic column.
- Instantaneous equilibrium on the wall pore surface.
- Isothermal operation.

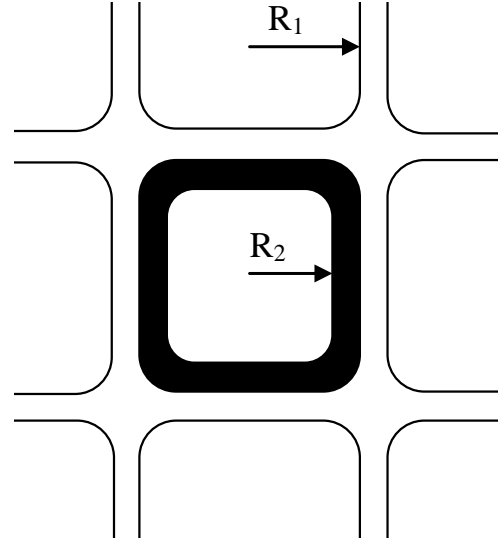


Fig. 1. The sketch of monolithic structure

In this work, an axially dispersed plug flow model through the channel is developed. Adsorption equilibrium is included in the model by using linear isotherm.

Mass balance in bulk phase in monolith column

Mass balance in the monolithic channel ($t > 0$; $0 \leq r \leq R_2$) can be calculated as

$$\frac{\partial C}{\partial t} = -V_z \frac{\partial C}{\partial z} + D_{ax} \frac{\partial^2 C}{\partial z^2} - \frac{(1 - \epsilon_b)}{\epsilon_b} \frac{1}{K} \frac{\partial \bar{C}_p}{\partial t} \quad (1)$$

where C is the liquid bulk phase concentration, \bar{C}_p is average pore concentration in the skeleton wall, z is the axial coordinate, t is time, and D_{ax} is the axial dispersion coefficient [4, 10, 11]. The initial and boundary conditions for Eq. (1) are as following:

Initial condition

$$t = 0; \quad C = 0 \quad \text{for all } z \quad (2)$$

Boundary conditions

$$z = 0; \quad C = C_F \quad t > 0 \quad (3)$$

$$z = L; \quad \frac{dC}{dz} = 0 \quad t > 0 \quad (4)$$

Mass balance in channel wall

The mass balance in channel wall is given as

$$D_p \frac{\partial}{\partial r} \left(r \frac{\partial C_p}{\partial r} \right) = \varepsilon_p \frac{\partial C_p}{\partial t} + \frac{\partial \bar{q}}{\partial t} \quad (5)$$

for $t > 0$; $R_2 \geq r \leq R_1$

The initial and Boundary conditions are:

Initial condition

$$t = 0; \quad C_p = 0 \quad \text{for all } r \quad (6)$$

Boundary conditions

$$r = R_2; \quad C_p|_{R_2} = C|_{R_2} \quad (7)$$

$$r = R_1; \quad \frac{\partial C_p}{\partial r} \Big|_{R_1} = 0 \quad (8)$$

where C_p is the liquid concentration in the wall pores and \bar{q} is the average wall adsorbed phase concentration. D_p is the wall pore diffusivity. If transport within the macro-pores occurs only by molecular diffusion, the D_p is given by

$$D_p = \frac{D_m}{\tau} \quad (9)$$

where D_m is the molecular diffusivity and τ is the wall pore tortuosity. For straight, randomly oriented, cylindrical pores, τ can be taken as 3 [12].

The adsorption equilibrium on the wall pore surface is described by linear adsorption isotherm:

$$q = KC_p \quad (10)$$

Averaging the pore concentration over the monolith wall and assuming the parabolic pore concentration profile through the wall, Eq. (5) is transformed in linear driving force (LDF) equation form:

$$(\varepsilon_p + K) \frac{\partial \bar{C}_p}{\partial t} = k_{LDF} (C|_{R_2} - \bar{C}_p) \quad (11)$$

where k_{LDF} is the internal mass transfer coefficient:

$$k_{LDF} = \frac{8D_p R_2^2}{(R_1^2 - R_2^2)^2} \quad (12)$$

Numerical simulation

The model set of partial differential equations (PDEs) was solved by using MATLAB 6.5. The PDEs were discretised in the spatial domain with the method of orthogonal collocation (OC). Detailed information on the method of OC can be found in [13-15]. The resulting set of ordinary differential equations (ODEs) was solved by using MATLAB subroutine ODE15s.

Validation of the discretisation method

The OC method is first used to simulate a case of heat conduction for which analytical equation can be obtained. It uses a polynomial of order 50. The equation for the transient heat conduction is given as:

$$\frac{\partial T}{\partial t} = \alpha_h \frac{\partial^2 T}{\partial z^2} \quad (13)$$

where α_h is the thermal diffusivity ($\text{m}^2 \text{s}^{-1}$), T is the temperature inside the slab ($^{\circ}\text{C}$), t is time (s) and z is the axial co-ordinate (m).

Heat conduction in a slab of thickness $2L$

A slab with thickness $2L = 3.0 \times 10^{-2}$ m, $\alpha_h = 5.0 \times 10^{-6} \text{ m}^2 \text{ s}^{-1}$ and initial temperature $T_{initial} = 1000 \text{ }^{\circ}\text{C}$ is suddenly immersed into an ice bath of $0 \text{ }^{\circ}\text{C}$. The temperature profile inside the slab in this case is symmetric. The boundary conditions are

$$T|_{z=0} = 0; \quad \frac{\partial T}{\partial z} \Big|_{z=L} = 0 \quad (14)$$

The analytical solution is given as [9]:

$$T = \frac{4T_{initial}}{\pi} \sum_{n=0}^{\infty} \frac{1}{(2n+1)} \exp\left(\frac{-\alpha_h(2n+1)^2 \pi^2 t}{(2L)^2}\right) \sin \frac{(2n+1)\pi z}{2L} \quad (15)$$

Figure 2 shows T as a function of dimensionless length (z/L), calculated using OC. Excellent agreement is obtained.

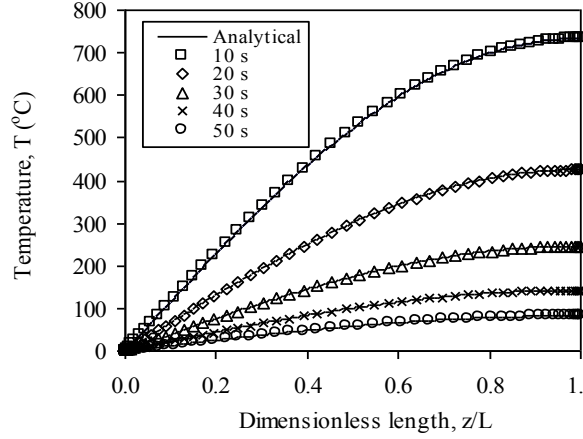


Fig. 2. Comparison of the numerical calculations and analytical solution of heat conduction in a slab of thickness $2L$

Validation of column model

The simulation programs are validated by simplifying a case of packed bed adsorber to compare the numerical calculation with analytical solution. The equations describing the packed bed adsorber are:

$$V_0 \frac{\partial C}{\partial z} + \varepsilon_b \frac{\partial C}{\partial t} + (1 - \varepsilon_b) \frac{\partial \bar{q}}{\partial t} = 0 \quad (16)$$

where

$$\frac{\partial \bar{q}}{\partial t} = k_{LDF} (q^* - \bar{q}) \quad (17)$$

q^* is the adsorption equilibrium on solid phase. It is equivalent to q in equation (10).

Initial conditions and boundary conditions are

$$C(0, \xi) = 0 \quad (18)$$

$$C_p(0, \xi) = 0 \quad (19)$$

$$C|_{\xi=0} = C_F \quad (20)$$

$$\frac{\partial C}{\partial \xi} \Big|_{\xi=1} = 0 \quad (21)$$

The analytical solution for equation (16) - (18) are given by Rice and Do (1995) as

$$\frac{C}{C_0} = J(\zeta, \eta) \quad (22)$$

where $J(\zeta, \eta)$ is defined as

$$J(\zeta, \eta) = 1 - e^{-\tau} \int_0^{\zeta} e^{-t} I_0(2\sqrt{\eta \cdot t}) dt \quad (23)$$

$$\text{where } \zeta = \left(\frac{k_c a}{\varepsilon_b} \right) \cdot \frac{z}{V_z} \quad (24)$$

$$\eta = \left[\frac{k_c a}{K(1 - \varepsilon_b)} \right] \cdot \left(t - \frac{z}{V_z} \right) \quad (25)$$

where $k_c a$ is the mass transfer constant (s^{-1}), ε_b is bed porosity, z is bed length (m), and t is time (s), and V_z is interstitial velocity (ms^{-1}). Input parameters for validation of column are given in Table 1. Time as function dimensionless concentration (C/C_0) is shown in Figure 3. Excellent agreement between the simulation and analytical solution is obtained as well.

Table 1. Input parameter for validation of packed bed adsorber model [14].

Input Parameter	Value	Unit
Column height, L	1.0	m
Bulk porosity, ε_b	0.4	-
Linear adsorption constant, K	2.0	-
Mass transfer constant, $k_c a$	0.1	s^{-1}
Superficial velocity, V_0	0.04	$m \cdot s^{-1}$
Linear driving force constant, $k_{LDF} = [k_c a / K(1 - \varepsilon_b)]$	0.083	s^{-1}
Interstitial velocity, $V_z = V_0 / \varepsilon_b$	0.1	$m \cdot s^{-1}$

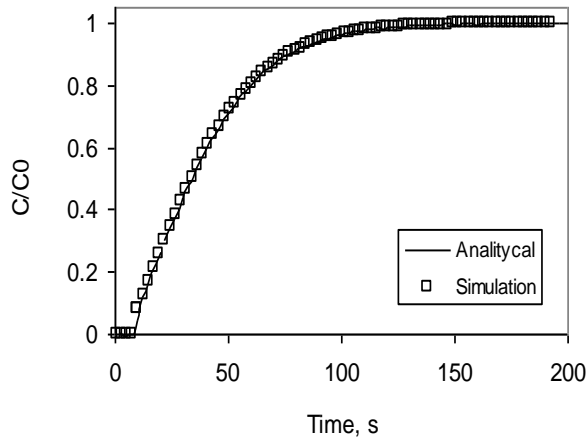


Fig. 3. Comparison of the numerical calculations using *OC* method and analytical solution of a packed bed adsorber

RESULT AND DISCUSSION

Figure 4 presents the simulation result of the breakthrough profiles for plug flow velocity profile obtained using data from [4] with 200 *cp*si monoliths having total length of 5 cm, 10 cm, 15 cm are plotted. The longer the total length of the monolith, the higher a displacement of breakthrough time value. The adsorption performance however remains identical. It can also be explained that short diffusion length occurs in the monolith. An additional advantage of activated carbon coated on monolith compare to carbon packed beds is the low pressure drop that monoliths produce in the system [3]. The pressure drop associated with the monolithic system was estimated by using the Hagen-Poiseuille equation. The value in this operation conditions is 2.8 Pa/m [3], while the pressure drop for a carbon packed bed calculated by the dimensionless friction factor using Chilton-Colburn correlations [12] gave a value of around 150 Pa/m.

The breakthrough curves for different velocity 1, 3, and 5 cm/s are presented in Figure 5. The slope of breakthrough curve for the velocity 1 cm/s decreases gradually. It is clear that there is no constant pattern behavior for the monolithic column. The effect of velocity which contributes to axial

mixing is lumped together into the axial dispersion coefficient.

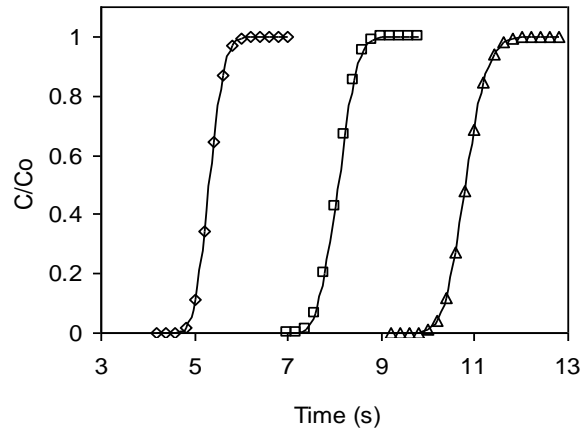


Fig. 4. Breakthrough profiles for monolith having 200 *cp*si at v 1 cm/s ($\diamond=5$ cm; $\square=10$ cm; $\Delta=15$ cm)

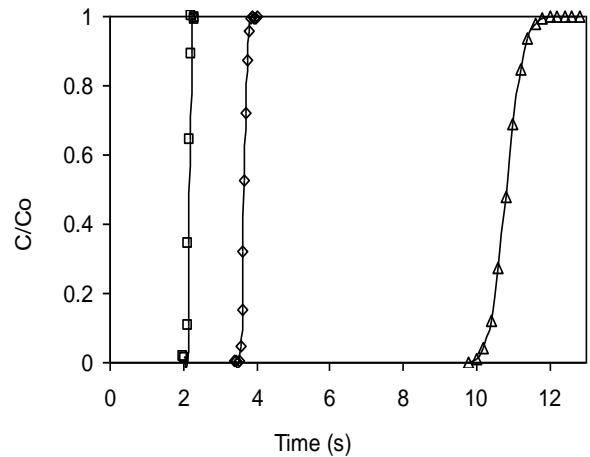


Fig. 5. Breakthrough profiles for monolith having 200 *cp*si at length 10 cm and different velocities ($\Delta=1$ cm/s; $\diamond=3$ cm/s; $\square=5$ cm/s).

CONCLUSION

The breakthrough curves shown by monoliths are very sharp and it gives extremely low pressure drop. It also shows that dynamic adsorptive capacity behavior of monolith column was very good. Monoliths are a promising alternative for the adsorption system. The width of the breakthrough profile scales with respect to the length of monolith takes place, if a laminar flow is over the channel. This case can be reduced by increasing the cell density.

NOMENCLATURE

C	bulk liquid phase concentration (kg/m ³)
C_p	liquid concentration in the skeleton pores (kg/m ³)
\bar{C}_p	average concentration in the skeleton pores (kg/m ³)
C_F	initial (feed) concentration (kg/m ³)
D_{ax}	axial dispersion coefficient (m ² /s)
D_m	molecular diffusion (m ² /s)
D_p	pore diffusion (m ² /s)
k_{LDF}	linear driving force mass transfer coefficient (1/s)
K	linear adsorption constants
$k_c a$	mass transfer constant (s ⁻¹)
L	length of the monolithic column (m)
q	equilibrium adsorbed phase concentration in the monolithic skeleton (kg/m ³)
q^*	equilibrium adsorbed phase concentration in packed bed (kg/m ³)
r	radial variable (m)
R_1	radius of the channel's skeleton wall (m)
R_2	radius of the channel (m)
t	time variable (s)
T	temperature (K)
V_0	superficial velocity (ms ⁻¹)
V_z	interstitial velocity (ms ⁻¹)
z	axial variable (m)
<i>Greek letters</i>	
α_h	thermal diffusivity (m ² s ⁻¹)
ε_b	bulk porosity
ε_p	internal porosity
τ	skeleton pore tortuosity

REFERENCES

1. Irandoust, S. and B. Andersson, 1989. Liquid Film in Taylor Flow Through a Capillary, *Ind. Eng. Chem. Res.*, 28 (11): 1684 – 1688.
2. Gadkaree, K.P., 1998. Carbon honeycomb structure for adsorption application, *Carbon*, 36: 981-989.
3. Cybulski, A. and J.A. Moulijn, 1994. Monoliths in heterogeneous catalysis, *Catal. Rev. Sci. Eng.* 36 (2): 179-270.
4. Valdes-Solis, T., M.J.G. Linders, F. Kapteijn, G. Marban, and A.B. Fuertes, 2004. Adsorption and breakthrough performance of carbon coated ceramic monoliths at low concentration of n-butane. *Chem. Eng. Sci.*, 59: 2791-2800.
5. Williams, J.L., 2001. Monolith structure, materials, properties and uses, *Catal. Today*, 69: 3-9.
6. Yates, M., J. Blanco, P. Avila, M.P. Martin, 2000. Honeycomb monoliths of activated carbons for effluent gas purification. *Micropor. Mesopor. Mater.*, 37: 201-208.
7. Irandoust, S., B. Andersson, E. Bengtsson and M. Silverstrom, 1989. Scaling up of a monolithic Catalyst reactor with two phase flow. *Ind. Chem. Res.*, 28: 1489 – 1493.
8. Edvinsson, A. R., M. Nystrom, Siverstrom, A. Sellin, A.C. Delive, U. Andersson, W. Herrmann and T. Berglin, 2001. Development of a monolith-based process for H₂O₂ production: from idea to large scale implementation. *Catal. Today* 69: 247-252.
9. Carslaw, H.S. and Jaeger, J.C., 1986. *Conduction of Heat in Solid*. 2nd Edition, Clarendon Press, Oxford, p. 96.
10. Gritti, F., W. Piatkowski and G. Guiochon, 2002. Comparison of the adsorption equilibrium of a few low molecular mass compounds on a monolithic and a packed column in reversed phase liquid chromatography. *Journal of Chromatography A.*, 978: 81-107.
11. Zabka, M., Minceva, M., and Rodrigues, A.E., 2006. Experimental and Modeling Study of Adsorption in

- Preparative Monolithic Silica Column. Chem. Eng. and Proc., 45: 150-160.
12. Rutven, D.M., 1984. Principles of Adsorption and Adsorption Processes, John Wiley & Sons Inc., New York. pp. 206-208.
 13. Villadsen, J. and M.L. Michelsen, 1978. Solution of Differential Equation Model by Polynomial Approximation. Prentice-Hall, Inc., Englewood Cliffs, pp. 92-98.
 14. Rice, R.G. and D.D. Do, 1995. Applied Mathematics and Modeling For Chemical Engineers. John Wiley & Sons, Inc., New York, p. 311.
 15. Choong, T.S.Y., 2000. Algorithm synthesis for modeling cyclic processes: rapid pressure swing adsorption. Ph.D. Thesis, The University of Cambridge, United Kingdom, pp. 57-62.